Chinese Chemical Letters 36 (2025) 110296

Contents lists available at ScienceDirect

Chinese Chemical Letters

journal homepage: www.elsevier.com/locate/cclet

Direct identification of energy transfer mechanism in Ce^{III}-Mn^{II} system by constructing molecular heteronuclear complexes

Huanyu Liu[1], Gang Yu[1], Ruoyao Guo, Hao Qi, Jiayin Zheng, Tong Jin, Zifeng Zhao, Zuqiang Bian, Zhiwei Liu*

Beijing National Laboratory for Molecular Sciences, State Key Laboratory of Rare Earth Materials Chemistry and Applications, College of Chemistry and Molecular Engineering, Peking University, Beijing 100871, China

ARTICLE INFO

Article history:
Received 30 April 2024
Revised 18 July 2024
Accepted 24 July 2024
Available online 26 July 2024

Keywords:
Dipole-quadrupole interaction
Förster resonance energy transfer
Manganese complex
Cerium complex
Photoluminescence

ABSTRACT

Sensitization of metal-centered forbidden transitions is of great significance. Solid Mn^{II}-based phosphors with d-d forbidden transition sensitized by Ce^{III} with d-f allowed transition are promising light conversion materials, but the energy transfer mechanism in Ce^{III}-Mn^{II} is still in dispute for the uncertainty of distances between metal centers. Herein, for the first time, we explored the energy transfer mechanism in two well-designed luminescent heteronuclear complexes with clear crystal structures, *i.e.*, Ce-N8-Mn and Ce-N2O6-Mn (N8 = 1,4,7,10,13,16,21,24-octaazabicyclo[8.8.8]hexacosane; N2O6 = 4,7,13,16,21,24-hexaoxa-1,10-diazabicyclo[8.8.8]hexacosane). Short distances between metal centers facilitate efficient energy transfer from Ce^{III} to Mn^{II} in both complexes, resulting in high photoluminescence quantum yield up to unity. After systematic study of the two heteronuclear complexes as well as two reference complexes $Ce(N8)Br_3$ and $Ce(N2O6)Br_3$, we concluded that dipole-quadrupole interaction is the dominant energy transfer mechanism in the heteronuclear complexes.

During the development of phosphors with metal-centered emission from electric dipole forbidden transitions, including f-f transitions and d-d transitions, many phosphors with co-doped sensitizer and activator ions have been designed to pursue a higher color rendering index in lighting and a larger color gamut in display [1-4]. Trivalent cerium ion (Ce^{III}) is a typical sensitizer ion with absorption bands from spin- and parity-allowed f-d transition, and has been widely applied in phosphors containing divalent manganese ion (Mn^{II}) to enhance the Mn^{II}-center emission from spin- and parity-forbidden d-d transition through energy transfer (ET) (Scheme 1a) [5-11]. Since effective ET is crucial to achieve a high photoluminescence quantum yield (PLQY) and a predictable emission spectrum, exploration of the ET mechanism is of great importance [12-15]. However, though much work on the ET mechanism in Ce^{III}-Mn^{II} solid phosphors has been reported, no consistent conclusion has been achieved. A dipole-quadrupole (dq) interaction mechanism was proposed in most cases [8,9,16-27] but dipole-dipole (dd) interaction [11,28-31] and exchange (ex) interaction [7,32-34] were also accounted to be the dominant mechanisms.

Dexter's theory elucidates the relations between the ET probability and the distance between the donor and the acceptor under different mechanisms [35]. Because the distance between Ce^{III} and Mn^{II} in solid phosphors could not be definitely measured, an indirect parameter, *i.e.* concentration (*C*), is utilized as the substitute to build the correlation with the ET efficiency (Scheme 1b). The ET efficiency is usually represented by overall parameters like emission intensities [9] and weighted-average lifetimes [34] of Ce^{III}. And the identification of the ET mechanism in Ce^{III}-Mn^{II} is usually carried out following this indirect method firstly proposed by Reisfeld [36]. Naturally, one would wonder about investigating the ET mechanism based on the direct method with a parameter of the distance between Ce^{III} and Mn^{II}. Inspired by a heteronuclear Eu^{II}-Mn^{II} complex in our previous work [37], we realized that luminescent heteronuclear Ce^{III}-Mn^{II} complexes have clear and definite distances between Ce^{III} and Mn^{II} and could provide an ideal platform for the investigation on the ET mechanism (Scheme 1c).

On the construction of luminescent heteronuclear Ce^{III}-Mn^{II} complexes, macrocyclic ligands with size selectivity were chosen to build chelate cations containing Ce^{III} while green-emitting $MnBr_4^{2-}$ acted as the anion, considering the significant difference between the radii of Ce^{III} (114 pm) and Mn^{II} (67 pm) [38]. The chosen ligands, N8 (1,4,7,10,13,16,21,24-octaazabicyclo[8.8.8]hexacosane) and N2O6 (4,7,13,16,21,24-

* Corresponding author.
E-mail address: zwliu@pku.edu.cn (Z. Liu).
[1] These authors contributed equally to this work.

https://doi.org/10.1016/j.cclet.2024.110296
1001-8417/

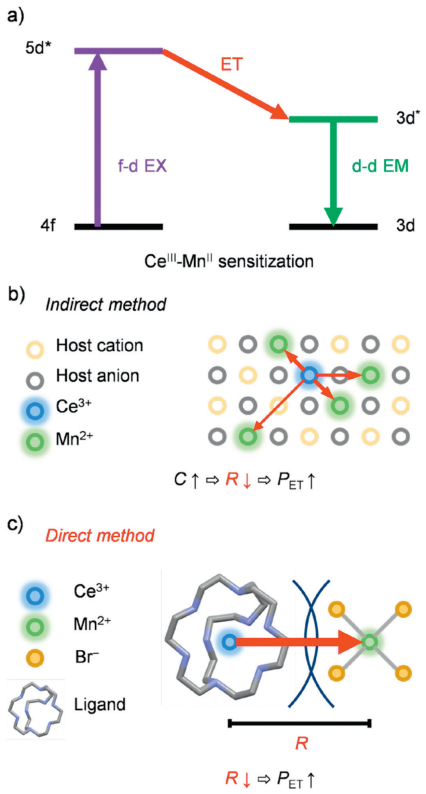

Scheme 1. (a) The schematic diagram of Ce^{III}-Mn^{II} sensitization; EX, excitation, EM, emission, ET, energy transfer. (b) The indirect method and (c) the direct method for identifying the ET mechanism in Ce^{III}-Mn^{II}; *C*, concentration; *R*, distance; P_{ET}, energy transfer probability.

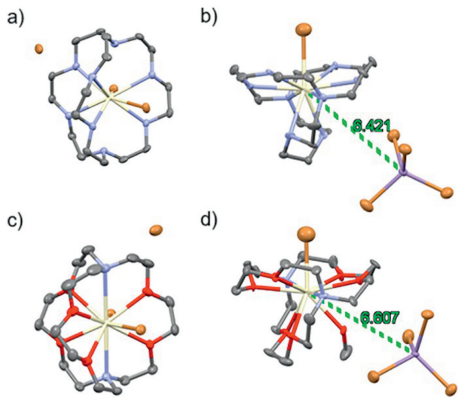

Fig. 1. Molecular structures of (a) $Ce(N8)Br_3$, (b) Ce-N8-Mn, (c) $Ce(N2O6)Br_3$, and (d) Ce-N2O6-Mn. Thermal ellipsoids are drawn at 50% probability. Hydrogen atoms and the solvent molecules are omitted for clarity. The distances (Å) between Ce^{III} and Mn^{II} in Ce-N8-Mn and Ce-N2O6-Mn were marked in green. It should be noted that $Ce(N2O6)Br_3$ has two similar types of structures in one asymmetry unit (Fig. S3) and only one type is exhibited here for concision. Color scheme: C, black; N, blue; O, red; Ce, yellow; Mn, purple; Br, orange.

hexaoxa-1,10-diazabicyclo[8.8.8]hexacosane), also provide rigid coordination environment to protect Ce^{III} from non-radiative decay pathways. Based on this, complex Ce-N8-Mn and complex Ce-N2O6-Mn were designed and synthesized. In order to estimate the lifetimes and emission spectra of Ce^{III} with similar coordination environment while free of inter-metal-centered ET, two control complexes, $Ce(N8)Br_3$ and $Ce(N2O6)Br_3$, were also prepared. Based on systematic characterizations and analysis of these complexes, dipole-quadrupole interaction was proposed to dominate the ET mechanism in Ce^{III}-Mn^{II}.

Ligand N8 can be facilely synthesized following previous reported routes [39] and ligand N2O6 is commercially available. $Ce(N8)Br_3$ was synthesized by mixing ligand N8 and $CeBr_3$ in methanol and Ce-N8-Mn was crystalized from the mixture solution of $Ce(N8)Br_3$ and $MnBr_2$ in methanol. $Ce(N2O6)Br_3$ and Ce-N2O6-Mn were prepared similarly. The chemical composition and purity were confirmed by elemental analysis and single crystal X-ray diffraction. More details about synthesis were shown in Supporting information.

Single crystals of $Ce(N8)Br_3$, Ce-N8-Mn, $Ce(N2O6)Br_3$, and Ce-N2O6-Mn suitable for X-ray diffraction test were obtained by evaporation crystallization. Acetonitrile, dichloromethane and methanol were suitable for $Ce(N8)Br_3$, $Ce(N2O6)Br_3$ and two heteronuclear complexes, respectively. $Ce(N8)Br_3$ crystalizes in a triclinic space group of $P\bar{1}$ and shows ten-coordinated geometry where two Br^- ions coordinate directly to Ce^{III} and the last one acts as a counterion (Fig. 1a, Table S1 and Fig. S1 in Supporting information). When $MnBr_2$ is introduced, the counterion Br^- and one of coordinated Br^- are seized to build $MnBr_4^{2-}$. As a result, the coordination number of Ce^{III} decreases to nine in Ce-N8-Mn (Fig. 1b, Table S2 and Fig. S2 in Supporting information). In Ce-N8-Mn with an orthorhombic space group of $P2_12_12_1$, the average bond length of Mn-Br is 2.465 Å and the minimum distance between Ce^{III} and neighboring Mn^{II} is 6.421 Å. $Ce(N2O6)Br_3$ shares similar coordination geometry with $Ce(N8)Br_3$ but crystalizes in a monoclinic space group of $P2/n$ (Fig. 1c, Table S3 and Fig. S3 in Supporting information). Unlike Ce-N8-Mn, Ce-N2O6-Mn maintains ten-coordinated geometry of Ce^{III} with one methanol molecule as an inner ligand and crystalizes in a monoclinic space group of $P2_1$ (Fig. 1d, Table S4 and Fig. S4 in Supporting information). The preference for ten-coordinated geometry of Ce-N2O6-Mn could be attributed to the lack of hindrance in N2O6, as that brought by N–H bonds in ligand N8. In Ce-N2O6-Mn, the average bond length of Mn-Br is 2.476 Å and the minimum distance between Ce^{III} and neighboring Mn^{II} is 6.607 Å. Both parameters become a little larger compared to those in Ce-N8-Mn, which results from the larger volume of the cation with a coordinating methanol molecule (Fig. S5 in Supporting information). Similarly, the shortest distance between two Mn^{II} ions also lengthens from 7.651 Å in Ce-N8-Mn to 8.783 Å in Ce-N2O6-Mn.

Ce-N8-Mn exhibits dual emission in solid state, with a dominant emission peaking at 523 nm and a full width at half maximum of 62 nm (Fig. 2a and Table S5 in Supporting information). The lifetime (τ) of this peak is 304 μs (Fig. 2b), indicating that this green emission originates from the spin- and parity-forbidden $^4T_2 \rightarrow {}^6A_1$ transition of Mn^{II} in $MnBr_4^{2-}$ [40-42]. The weak emission at blue region displays remarkably double-peak characteristics and the higher of the two peaks centers at 424 nm (Fig. S6a in Supporting information). This double-peak emission has a mono-exponential decay lifetime of 1.04 ns (Fig. 2c and Fig. S6b in Supporting information), which is much shorter than that of the green emission. From the double-peak profile and the ns-level short lifetime, one can attribute this blue emission to the parity-allowed $5d \rightarrow 4f$ transition of Ce^{III} [43-46]. This identification is further supported by the emission spectrum and the lifetime of $Ce(N8)Br_3$ in solid state (the maximum emission wavelength $\lambda_{max} = 408$ nm and $\tau = 56.2$ ns, Figs. 2a and c, and Fig. S6c in Supporting information).

Under the aforementioned ascription of emission peaks, the overlap between the excitation spectra of Mn^{II}-center emission and those of Ce^{III}-center emission in the region of 250–400 nm indicates an ET from Ce^{III} to Mn^{II} in Ce-N8-Mn (Fig. 2d and Fig. S6d in Supporting information). The excitation peaks near 450 nm could be ascribed to the $^6A_1 \rightarrow {}^4A_1/{}^4E(G)$ (436 nm), $^4T_2(G)$ (451 nm), and $^4T_1(G)$ (472 nm) transitions of Mn^{II} and stand for the direct excitation [47,48]. The overlap under 400 nm means excited states on

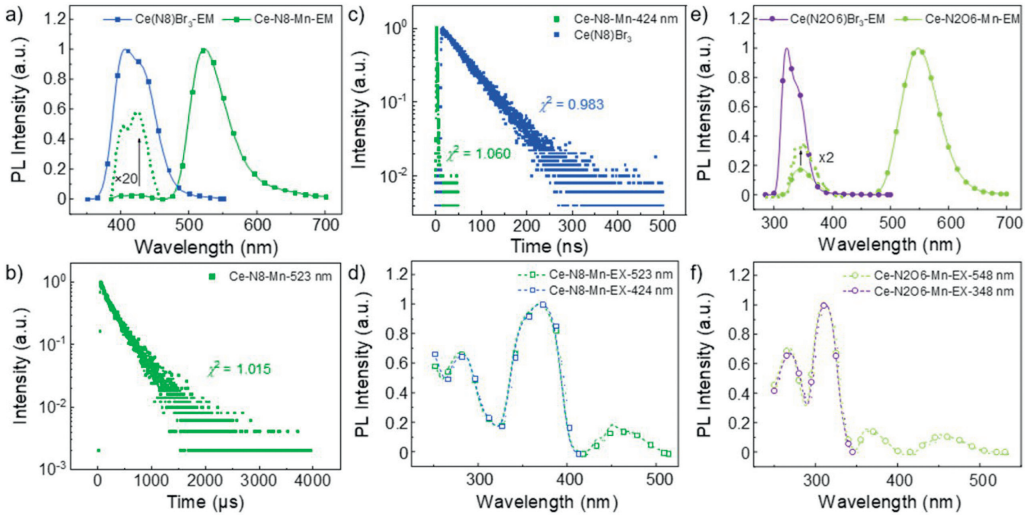

Fig. 2. (a) Emission spectra of Ce-N8-Mn and $Ce(N8)Br_3$. (b) Emission decay curve of Mn^{II}-center emission in Ce-N8-Mn. (c) Emission decay curves of Ce^{III}-center emission in Ce-N8-Mn and $Ce(N8)Br_3$. (d) Excitation spectra of Ce-N8-Mn. (e) Emission spectra of Ce-N2O6-Mn and $Ce(N2O6)Br_3$. (f) Excitation spectra of Ce-N2O6-Mn. For Ce-N8-Mn and Ce-N2O6-Mn, the detecting wavelengths of emission decay curves and excitation spectra were marked in the legend.

Ce^{III} could relax to the emission state on Mn^{II}. In other words, energy could be transferred from Ce^{III} to Mn^{II}. This conclusion is further confirmed by the shorter lifetime of Ce^{III}-center emission in Ce-N8-Mn compared with that in $Ce(N8)Br_3$ (1.04 ns *vs.* 56.2 ns), because the emergence of ET accelerates the overall deactivation process of the emission state on Ce^{III}.

Similar conclusions as aforementioned could be obtained on Ce-N2O6-Mn and $Ce(N2O6)Br_3$ (Figs. 2e and f, Fig. S7 and Table S5 in Supporting information), and only some differences would be discussed here for clarity. First of all, because longer average bond length of Mn-Br weakens the coordinating field in $MnBr_4^{2-}$, the Mn^{II}-center emission in Ce-N2O6-Mn is a little red-shifted (548 nm, Fig. S8 in Supporting information). In contrast, Ce-N2O6-Mn and $Ce(N2O6)Br_3$ show remarkably blue-shifted Ce^{III}-center emission (348 nm and 322 nm) for O atom produces weaker coordinating field than N atom does. As a result, the excitation spectra of Mn^{II}-center emission in Ce-N2O6-Mn contain more direct excitation peaks ($^6A_1 \rightarrow {}^4T_1(P)$ (362 nm) and $^4E(D)$ (373 nm)). Another noteworthy feature about the emission spectrum of Ce-N2O6-Mn is that the relative intensity of Ce^{III}-center emission is much stronger, which means the ET process is less complete.

Thanks to the compact protection brought by macrocyclic ligands, both $Ce(N8)Br_3$ and $Ce(N2O6)Br_3$ have a near-unity PLQY (Table S5). When the whole emission spectra are integrated, the PLQY of Ce-N8-Mn is 62% whereas the PLQY of Ce-N2O6-Mn is about 100%. Considering the almost 100% PLQYs of mononuclear complexes $Ce(N2O6)Br_3$ and $Ce(N8)Br_3$, which mean the non-radiative transition processes on the Ce^{III} centers are negligible, this difference on PLQY originates most likely from the Mn^{II} centers (Fig. S9 in Supporting information). This conclusion is further supported by the differences on lifetime (304 μs *vs.* 567 μs). According to literature [49,50], the higher PLQY of Ce-N2O6-Mn is caused by the longer distance between two adjacent Mn^{II} centers (8.783 Å *vs.* 7.651 Å in Ce-N8-Mn). As a new example of Mn-containing complex with recording PLQY, Ce-N2O6-Mn reveals the feasibility of 4f-3d sensitization for the design of highly luminescent metal complexes with forbidden d-d transitions.

Based on aforementioned characterizations, the ET mechanism in heteronuclear Ce^{III}-Mn^{II} complexes was investigated as follows. Firstly, under the assumption that the dominant mechanisms are dd, dq, and ex interaction, respectively, we would separately calculate the theoretical ratio of ET probability in Ce-N8-Mn to that in Ce-N2O6-Mn. Then, we would compare these calculated results with the experimental result and draw a conclusion.

According to Dexter's theoretical analysis [35], the ET probability of dd interaction ($P_{ET}(dd)$) could be strictly expressed (Eq. S1 in Supporting information). However, in systems with the same acceptor ($MnBr_4^{2-}$) and different donors, the following simplified relation is sufficient for discussion (Eqs. 1 and 2)

$$P_{ET}(dd) \propto F_c \cdot \frac{1}{R^6} \cdot \frac{1}{\tau_d} \quad (1)$$

① F_c stands for the overlap integral between the emission spectra of the donor ($f_d(E)$, normalized) and the absorption spectra of the acceptor ($F_a(E)$, normalized) and has the formula as

$$F_c = \int \frac{f_d(E)F_a(E)}{E^4} dE \quad (2)$$

In our system, the $f_d(E)$ of Ce^{III} in the heteronuclear complex is estimated by the emission spectrum profile of the mononuclear complex and the $F_a(E)$ of Mn^{II} is estimated by the excitation spectrum profile of a reported Sr^{II}-Mn^{II} complex without energy donors (Fig. S10 in Supporting information) [37]. Since originating from the same d-d transitions, the excitation spectra of luminescent $MnBr_4^{2-}$ salts have similar profiles and contain nearly the same information as the absorption spectra do. Thus, it is reasonable to estimate the $F_a(E)$ with the excitation spectra. Herein, the Sr^{II}-Mn^{II} complex was selected for its structural similarity with Ce^{III}-Mn^{II} complexes and its ready-made spectrum data in literature. The convolution spectrum profiles (Fig. S11a in Supporting information) showed that more energy levels of Mn^{II} could be reached *via* ET in Ce-N8-Mn than in Ce-N2O6-Mn. Thus, the calculated F_c in Ce-N8-Mn (1.61×10^{-22}) is larger than that in Ce-N2O6-Mn (2.87×10^{-23}).

② R represents the distance between Ce^{III} and Mn^{II}. Herein, only the minimum distance between Ce^{III} and neighboring Mn^{II} was considered for the minimum distance represented the maximum ET probability and dominated the ET processes. According to the crystal structures, R in Ce-N8-Mn and Ce-N2O6-Mn were 6.421 Å and 6.607 Å, respectively.

③ τ_d is the lifetime of the donor without ET. Herein, τ_d was estimated by the lifetime of Ce^{III}-center emission in the mononuclear complex, which is 56.2 ns for $Ce(N8)Br_3$ and 19.8 ns for $Ce(N2O6)Br_3$.

Inserting the corresponding values of F_c, R and τ_d into Eq. 1, we got the calculated ratio of $P_{ET}(dd)$ in Ce-N8-Mn to $P_{ET}(dd)$ in

Ce-N2O6-Mn to be 2.35. This result indicates that if dd interaction was the dominant ET mechanism in Ce^{III}-Mn^{II}, the experimental ratio of ET probabilities of the two heteronuclear complexes should be close to 2.35.

For the dq interaction mechanism, the ET probability (P_{ET}(dq)) has a similar relation (Eq. 3):

$$P_{ET}(dq) \propto F_c \cdot \frac{1}{R^8} \cdot \frac{1}{\tau_d} \quad (3)$$

where the main difference is the power of R compared with Eq. 1.

In the same way, inserting the corresponding values of F_c, R and τ_d into Eq. 3 gave the calculated ratio of P_{ET}(dq) in Ce-N8-Mn to P_{ET}(dq) in Ce-N2O6-Mn to be 2.48. That is to say, if dq interaction was the dominant ET mechanism in Ce^{III}-Mn^{II}, the experimental ratio of ET probabilities of the two heteronuclear complexes should be close to 2.48.

The ET probability of exchange interaction (P_{ET}(ex)) could be estimated as follows (Eqs. 4 and 5).

$$P_{ET}(ex) \propto F_{ex} \cdot \exp\left(-\frac{2R}{l}\right) \quad (4)$$

where

$$F_{ex} = \int f_d(E) F_a(E) dE \quad (5)$$

and l represents the effective average Bohr radius for the excited states of Ce^{III} and the ground states of Mn^{II}. Herein, l was estimated to the value of 0.461 Å as reported in Ce^{III}-Mn^{II} *via* exchange interaction ET mechanism [32]. F_{ex} was calculated under the same condition as F_c and similar convolution spectrum profiles were obtained (Fig. S11b in Supporting information). The calculated F_c in Ce-N8-Mn and Ce-N2O6-Mn were 4.48×10^{-5} and 1.75×10^{-5}, respectively.

Likewise, inserting the corresponding values of F_{ex}, R and l into Eq. 4 gave the calculated ratio of P_{ET}(ex) in Ce-N8-Mn to P_{ET}(ex) in Ce-N2O6-Mn to be 5.75. If ex interaction was the dominant ET mechanism in Ce^{III}-Mn^{II}, the experimental ratio of ET probabilities should be close to 5.75.

In practice, the experimental ET probability (P_{ET}) is calculated as follows (Eq. 6).

$$P_{ET} = \frac{1}{\tau_{ET}} - \frac{1}{\tau_d} \quad (6)$$

where τ_{ET} and τ_d are the lifetimes of Ce^{III}-center emission in the heteronuclear complex and the mononuclear complex, respectively (Table S5). Apparently, other nonradiative processes are neglected. This approximation is reasonable because Ce-N2O6-Mn has a near-unity PLQY and light losses of Ce-N8-Mn are thought to happen on Mn^{II} as discussed above. The P_{ET} in Ce-N8-Mn and Ce-N2O6-Mn were $9.44 \times 10^8\ s^{-1}$ and $3.80 \times 10^8\ s^{-1}$, respectively. Thus, the experimental ratio of P_{ET} in Ce-N8-Mn to P_{ET} in Ce-N2O6-Mn was 2.48.

By comparing the experimental value (2.48) with the calculated theoretical values of three mechanisms (2.35, 2.48, and 5.75 for dd, dq, and ex interaction, respectively), one could find that the simulated result of dq interaction matched best (Fig. 3a). This result is consistent with our preliminary judgement of Förster resonance energy transfer in the Eu^{II}-Mn^{II} complex for the distance is too long for efficient ET *via* exchange interaction [37,51,52]. The dependence on R of P_{ET} (Fig. 3b, normalized at 6.607 Å) showed the different amplification extents of P_{ET} caused by the shortening of R from 6.607 Å to 6.421 Å. Though the numerical difference between dq interaction and dd interaction is small, the experiment reproduced the calculated theoretical result precisely. Therefore, we proposed that dipole-quadrupole interaction dominated the ET mechanism from Ce^{III} to Mn^{II}. It is worth noting that the ET mechanism would be different if the distances between metal centers

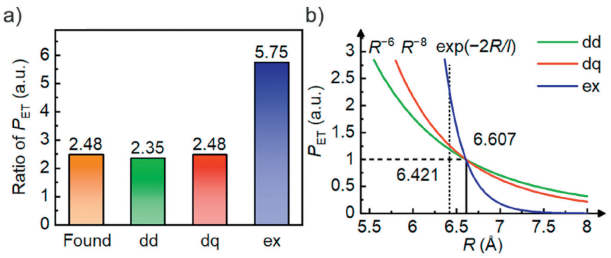

Fig. 3. (a) The experimental and calculated theoretical ratio of ET probability (P_{ET}) in Ce-N8-Mn to that in Ce-N2O6-Mn. (b) The dependence on the distance (R) of ET probability (P_{ET}); dd, dq, and ex stand for dipole-dipole, dipole-quadrupole, and exchange interaction, respectively.

are in different ranges. For example, in an inorganic system with Eu^{II}-Mn^{II} ET where many Eu^{II} centers only have slow ET processes caused by long distances, dd interaction was proposed [53].

In summary, we prepared two luminescent heteronuclear Ce^{III}-Mn^{II} complexes with macrocyclic ligands chelating Ce^{III} specifically. Both complexes exhibit efficient energy transfer from Ce^{III} to Mn^{II} and a near-unity PLQY was achieved in Ce-N2O6-Mn. This is the first time that Ce^{III}-Mn^{II} energy transfer was constructed and found in a molecular complex. Moreover, we proposed a new method in which direct correlations of the energy transfer probability to the distance, the spectral overlap integral, and the lifetime were taken as evidences of the energy transfer mechanism. By this way, dipole-quadrupole interaction mechanism was supported by the experimental data. One more time, this work demonstrated the feasibility of 4f-3d sensitization for preparing highly luminescent metal complexes with forbidden d-d transitions. The research method on the energy transfer mechanism in Ce^{III}-Mn^{II} developed here also brought the opportunity for the investigation of other energy transfer processes between metal centers.

Declaration of competing interest

The authors declare the following financial interests/personal relationships which may be considered as potential competing interests: A patent has been filed on this paper.

CRediT authorship contribution statement

Huanyu Liu: Writing – original draft, Methodology, Investigation, Conceptualization. **Gang Yu:** Writing – review & editing, Methodology, Funding acquisition. **Ruoyao Guo:** Investigation. **Hao Qi:** Investigation. **Jiayin Zheng:** Investigation. **Tong Jin:** Investigation. **Zifeng Zhao:** Funding acquisition. **Zuqiang Bian:** Writing – review & editing, Project administration, Funding acquisition. **Zhiwei Liu:** Writing – review & editing, Supervision, Project administration, Funding acquisition, Conceptualization.

Acknowledgments

The authors gratefully acknowledge the financial support from the National Key R&D Program of China (Nos. 2022YFB3503702, 2023YFB3506901, 2021YFB3501800) and the National Natural Science Foundation of China (Nos. 92156016, 62104013, 22071003).

Supplementary materials

Supplementary material associated with this article can be found, in the online version, at doi:10.1016/j.cclet.2024.110296.

References

[1] A.G. Bispo-Jr, L.F. Saraiva, S.A.M. Lima, A.M. Pires, M.R. Davolos, J. Lumin. 237 (2021) 118167.

[2] Y. Yang, K. Wang, D. Yan, Chem. Commun. 53 (2017) 7752–7755.
[3] Y. Yang, K. Wang, D. Yan, ACS Appl. Mater. Interfaces 9 (2017) 17399–17407.
[4] X. Yang, X. Lin, Y. Zhao, Y.S. Zhao, D. Yan, Angew. Chem. Int. Ed. 56 (2017) 7853–7857.
[5] J. Tang, J. Si, X. Fan, et al., J. Rare Earths 40 (2022) 878–887.
[6] R.J. Ginther, J. Electrochem. Soc. 101 (1954) 248.
[7] J.L. Patel, B.C. Cavenett, J.J. Davies, W.E. Hagston, Phys. Rev. Lett. 33 (1974) 1300–1303.
[8] C.H. Huang, T.W. Kuo, T.M. Chen, ACS Appl. Mater. Interfaces 2 (2010) 1395–1399.
[9] J. Zhang, X. Zhang, J. Zhang, et al., J. Mater. Chem. C 5 (2017) 12069–12076.
[10] J. Si, L. Wang, L. Liu, et al., J. Mater. Chem. C 7 (2019) 733–742.
[11] B. Zheng, X. Zhang, D. Zhang, et al., Chem. Eng. J. 427 (2022) 131897.
[12] B. Zhou, Z. Qi, M. Dai, C. Xing, D. Yan, Angew. Chem. Int. Ed. 62 (2023) e202309913.
[13] S. Feng, Y. Ma, S. Wang, et al., Angew. Chem. Int. Ed. 61 (2022) e202116511.
[14] B. Zhou, D. Yan, Adv. Funct. Mater. 29 (2019) 1807599.
[15] L. Wu, Y. Fang, W. Zuo, et al., JACS Au 2 (2022) 853–864.
[16] U. Caldiño, J. Phys.: Condens. Matter 15 (2003) 7127.
[17] M. Müller, T. Jüstel, J. Lumin. 155 (2014) 398–404.
[18] U. Caldiño, J.L. Hernández-Pozos, C. Flores, A. Speghini, M. Bettinelli, J. Phys.: Condens. Matter 17 (2005) 7297.
[19] U. Caldiño, J. Phys.: Condens. Matter 15 (2003) 3821.
[20] Y. Jia, Y. Huang, Y. Zheng, et al., J. Mater. Chem. 22 (2012) 15146–15152.
[21] D. Geng, G. Li, M. Shang, et al., J. Mater. Chem. 22 (2012) 14262–14271.
[22] G. Li, Y. Zhang, D. Geng, et al., ACS Appl. Mater. Interfaces 4 (2012) 296–305.
[23] J. Sun, J. Zeng, Y. Sun, H. Du, J. Lumin. 138 (2013) 72–76.
[24] M. Jiao, Y. Jia, W. Lü, et al., Dalton Trans. 43 (2014) 3202–3209.
[25] Z. Wang, S. Lou, P. Li, J. Lumin. 156 (2014) 87–90.
[26] X. Mi, J. Sun, P. Zhou, et al., J. Mater. Chem. C 3 (2015) 4471–4481.
[27] Y. Li, Z. Wang, M. Guan, et al., Mater. Res. Bull. 115 (2019) 105–115.
[28] L. Bian, T. Wang, Z. Song, et al., Chin. Phys. B 22 (2013) 077801.
[29] D. Pasiński, E. Zych, J. Sokolnicki, J. Alloy. Compd. 653 (2015) 636–642.
[30] R. Vishwanath, K. Munirathnam, R. Vijaya, P.C. Nagajyothi, J. Lumin. 215 (2019) 116651.
[31] J. Ding, M. Kuang, S. Liu, et al., Dalton Trans. 51 (2022) 9501–9510.
[32] N. El Jouhari, C. Parent, G. Le Flem, J. Solid State Chem. 123 (1996) 398–407.
[33] C. Guo, L. Luan, Y. Xu, F. Gao, L. Liang, J. Electrochem. Soc. 155 (2008) J310.
[34] M. Müller, S. Fischer, T. Jüstel, RSC Adv. 5 (2015) 67979–67987.
[35] D.L. Dexter, J. Chem. Phys. 21 (1953) 836–850.
[36] R. Reisfeld, E. Greenberg, R. Velapoldi, B. Barnett, J. Chem. Phys. 56 (1972) 1698–1705.
[37] G. Yu, H. Liu, W. Yan, et al., Mater. Horizons 10 (2023) 625–631.
[38] P. Atkins, T. Overton, J. Rourke, M. Weller, F. Armstrong, Shriver and Atkins' Inorganic Chemistry, 5th ed., Oxford University Press, Oxford, 2010.
[39] J. Li, L. Wang, Z. Zhao, et al., Nat. Commun. 11 (2020) 5218.
[40] Y. Qin, P. She, X. Huang, W. Huang, Q. Zhao, Coord. Chem. Rev. 416 (2020) 213331.
[41] P. Tao, S. Liu, W.Y. Wong, Adv. Opt. Mater. 8 (2020) 2000985.
[42] Y. Cheng, H. Ruan, Y. Peng, et al., Chin. Chem. Lett. 35 (2024) 108554.
[43] L. Wang, Z. Zhao, G. Zhan, et al., Light Sci. Appl. 9 (2020) 157.
[44] P. Fang, L. Wang, G. Zhan, et al., ACS Appl. Mater. Interfaces 13 (2021) 45686–45695.
[45] W. Yan, L. Wang, H. Qi, et al., Inorg. Chem. 60 (2021) 18103–18111.
[46] G. Blasse, G.J. Dirksen, N. Sabbatini, S. Perathoner, Inorg. Chim. Acta 133 (1987) 167–173.
[47] M.P. Davydova, L. Meng, M.I. Rakhmanova, et al., Adv. Opt. Mater. (2023) 2202811.
[48] L. Xu, X. Lin, Q. He, M. Worku, B. Ma, Nat. Commun. 11 (2020) 4329.
[49] V. Morad, I. Cherniukh, L. Pöttschacher, et al., Chem. Mater. 31 (2019) 10161–10169.
[50] L. Mao, P. Guo, S. Wang, A.K. Cheetham, R. Seshadri, J. Am. Chem. Soc. 142 (2020) 13582–13589.
[51] C. Xing, Z. Qi, B. Zhou, D. Yan, W. Fang, Angew. Chem. Int. Ed. 63 (2024) e202402634.
[52] R. Gao, D. Yan, Chem. Sci. 8 (2017) 590–599.
[53] J. He, N. Cai, L. Fu, R. Shi, Inorg. Chem. 61 (2022) 1745–1755.